by changes in the torsional potential term. Of primary importance is the selection of which torsions are included and which are excluded when there are multiple definitions for rotations about a particular bond. For any particular problem, various combinations of those definitions and various values of the rotational barrier heights can be used to search for the optimum overall potential. The gauche effect in O-C-C-O and O-C-C-C torsions can be used to fine tune the total potential and may be important in the differences between ribose and deoxyribose rings.[11]

Although Figures 9 and 12 indicate that our potential energy function is reasonable, it does not exactly reproduce the locations of the energy minima that are predicted from the combined results of crystallographic and NMR studies[10] and of other theoretical studies.[6,11,12] For example, our minimum energy configuration is at C4'-exo rather than C3'-endo, and the second minimum is at C1'-exo rather than C2'-endo. Further refinement of the potential is needed. Since a variety of methods[29-32] can be used to determine free energy differences, rather than just differences in internal energy, we believe that appropriate simulations would provide a very useful comparison of the various potential functions used to model ribose structure and dynamics. Such studies are now underway in this laboratory.

Acknowledgments. We thank Eric Westhof for comments on a preliminary version of this paper. This research was supported by grants from the National Science Foundation (PCM-84-17001) and the National Institutes of Health (GM-34015).

(33) **Note Added in Proof**: It has come to our attention that a relationship between P(CP) and P(AS) identical with eq 8 (except with an amplitude of 3°, rather than 4°) has been reported previously (de Leeuw, H. P. M., et al. *Isr. J. Chem.* **1980**, *20*, 108-126). Also, we should have mentioned two refinements to the Altona-Sundaralingam method: First, there is an averaging procedure[3,17] that eliminates the problems of choosing a reference atom described in our discussion following eq 2. With this procedure, "there is no difference between the AS and RWS results, except for roundoff errors" (Altona, C., personal communication). Second, eq 1 can be improved by the addition of a small phase angle ϵ_j (always less than 1.5° for ribose) and multiplication of θ_j by an amplitude factor a_j (ranging from 0.977 to 1.016 for ribose); values of the parameters and a full discussion are given by de Leeuw in the following: de Leeuw, F. A. M., et al. *J. Mol. Struct.* **1984**, *125*, 67-88.

Mechanism of Carbonyl Insertion Reaction of Pd and Pt Complexes. An ab Initio MO Study

Nobuaki Koga and Keiji Morokuma*

Contribution from the Institute for Molecular Science, Myodaiji, Okazaki, 444 Japan.
Received April 1, 1986

Abstract: The carbonyl insertion reaction of $Pd(CH_3)(H)(CO)(PH_3)$, **1**, and $Pt(CH_3)(H)(CO)(PH_3)$, **3**, has been studied by means of the ab initio MO method with the energy gradient. The transition state has been determined for the reaction of both **1** and **3**, which shows unequivocally that the reaction proceeds via methyl group migration. The reaction of **1** has a lower activation energy and is less endothermic than that of **3**. These differences can be ascribed to the difference of M-CH_3, M-CO, and M-$COCH_3$ bond strengths between the Pd and the Pt complexes, those in the Pt complexes being stronger than in the Pd complexes. Substitution by an electron-withdrawing fluorine on the alkyl group makes the metal-alkyl bond stronger and the activation barrier higher. An electron-releasing methyl substitution gives a reverse effect. A stronger trans effect makes the metal-carbon bond weaker to give a lower activation barrier.

The carbonyl insertion reaction 1 is one of the most important elementary organometallic reactions. This reaction has been implicated in various catalytic cycles as one of the key steps.[1] Many experimental studies have been carried out for better understanding of this important reaction.[2,3]

$$M(R)(CO)(L)_n \rightarrow M(COR)(L)_m \qquad (1)$$

There are several questions to be answered about this reaction. One central concern about the reaction mechanism has been the question whether (i) it is the alkyl group that migrates to the carbonyl group or (ii) it is the carbonyl group that migrates to insert into the metal-alkyl bond. One of the most elegant studies

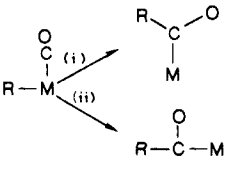

Scheme I

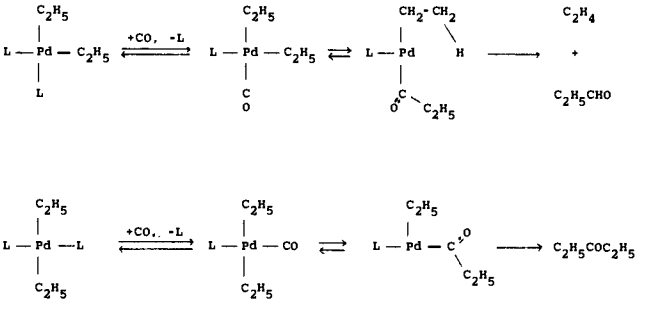

on this problem is that of $Mn(CH_3)(CO)_5$ by Noack and Calderazzo,[4] in which the reaction has been established to proceed via methyl group migration. In addition, the mechanism of carbonyl insertion reaction of rhodium,[5] iridium,[6] iron,[7] platinum,[8]

(1) See, for instance: Cotton, F. A.; Wilkinson, G. *Advanced Inorganic Chemistry*; Wiley: New York, 1980.
(2) Wojcicki, A. *Adv. Organomet. Chem.* **1973**, *11*, 87.
(3) (a) Calderazzo, F. *Angew. Chem., Int. Ed. Engl.* **1977**, *16*, 299. (b) Anderson, G. K.; Cross, R. J. *Acc. Chem. Res.* **1984**, *17*, 67.
(4) (a) Noack, K.; Calderazzo, F. *J. Organomet. Chem.* **1967**, *10*, 101. (b) Noack, K.; Ruch, M.; Calderazzo, F. *Inorg. Chem.* **1968**, *7*, 345. (c) Flood, T. C.; Jensen, J. E.; Statler, J. A. *J. Am. Chem. Soc.* **1981**, *103*, 4410.
(5) (a) Slack, D. A.; Egglestone, D. L.; Baird, M. C. *J. Organomet. Chem.* **1978**, *146*, 71. (b) Egglestone, D. L.; Baird, M. C.; Lock, C. J. L.; Turner, G. *J. Chem. Soc., Dalton Trans.* **1979**, 1576.
(6) Glyde, R. W.; Mawby, R. J. *Inorg. Chim. Acta.* **1971**, *5*, 317.

0002-7863/86/1508-6136$01.50/0

and palladium[9] complexes has been studied. In the reaction of $Fe(CH_3)(I)(CO)_2(P(CH_3)_3)_2$, only the methyl migration has been observed, while the dependence of reaction mechanism on the solvent has been found in some Fe complexes.[7]

In the case of the Pd complex, Ozawa and Yamamoto have concluded, based on the analysis of product distribution, that the alkyl group migration is the reaction mechanism.[9] They have studied the reaction of *cis*- and *trans*-$Pd(R)_2(L)_2$ ($R = CH_3, C_2H_5$, $L = PR'_3$) with CO. From the cis ethyl complex, ethylene and propanal were formed, and from the trans ethyl complex, 3-pentanone was produced. The ethyl group migration mechanism can explain the difference in the products, as shown in Scheme I. In the reaction of cis isomer, ethyl migration produces an acyl–alkyl intermediate, where the vacant site is located next to the ethyl group and thus β-elimination takes place easily to form ethylene, which is then followed by reductive elimination that gives propanal. On the other hand, in the acyl–alkyl intermediate of trans isomer, β-elimination reaction cannot take place; instead, reductive elimination gives 3-pentanone.

Due to the importance of the carbonyl insertion reaction in organometallic chemistry, studies have also been reported on the effects of the central metal, ligands, and alkyl group substituents. For instance, carbonyl insertion to a third-row transition-metal complex is slower than to a second-row transition-metal complex, and electron-withdrawing substituents on the migrating alkyl group make the reaction slower.[3]

Garrou and Heck have carried out a thorough investigation of the carbonyl insertion reaction of Ni, Pd, and Pt complexes.[10]

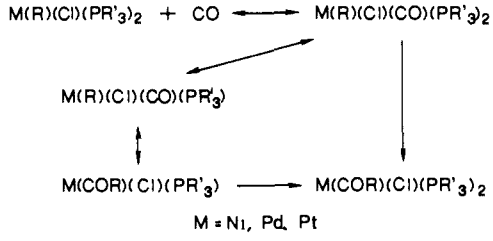

They have found that, in the presence of additional phosphine, carbonyl insertion takes place directly on a five-coordinate complex and that without additional phosphine the reaction passes through a four-coordinate intermediate. The latter reaction, which is the same as the reaction in Scheme I, is faster than the former direct reaction.

A few theoretical studies based on semiempirical and ab initio molecular orbital (MO) methods have been reported on the carbonyl insertion reaction.[11] Sakaki et al.[11a] used an ab initio MO method to study the following model reaction.

$$Pt(CH_3)(F)(CO)(PH_3) \rightarrow Pt(COCH_3)(F)(PH_3)$$

They changed the geometry of the reaction system stepwise to simulate three reaction paths: one for methyl migration, one for carbonyl migration, and one for the concerted migration of CO and methyl with simultaneous opening of the FPtP angle. From the energy change along the assumed paths, they concluded that methyl migration was the easiest and carbonyl migration was the most difficult. They, however, never determined the transition-state structure.

It is only in the last few years that ab initio molecular orbital determination of the transition state for elementary organometallic reactions has become practical. Among these reactions studied are oxidative addition/reductive elimination, β-elimination/olefin insertion, and isomerization of metallacycle to an alkylidene–olefin complex.[12] Since a transition state is hard to determine experimentally, a theoretical study could provide strong evidence on the reaction mechanism if it can establish the structure and the energy of the transition state of the reaction in question.

In the present paper, we report the results of an ab initio MO study of the carbonyl insertion reaction of the Pd and the Pt complex, eq 2 and 3, respectively. In **1** and **3**, the hydride is

$$M(CH_3)(H)(CO)(PH_3) \rightarrow M(COCH_3)(H)(PH_3) \qquad (2, 3)$$
1: M = Pd **2**: M = Pd
3: M = Pt **4**: M = Pt

located trans and CO cis to CH_3. We have determined the structure and the energy of the transition state as well as the reactant and the product. The transition state with a low activation energy has been found for methyl migration, and no transition state could be located for carbonyl migration. This portion of the work has been partly communicated.[13] Furthermore, we have investigated in detail the effects of the central transition metal, the alkyl group substituent, and the trans ligand on the structure of stationary points on the potential surface and on the rate and mechanism of carbonyl insertion reaction and clarified the theoretical origin of such effects.

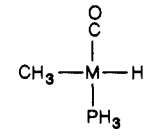

Method of Calculation

For the geometry optimization we used the restricted Hartree–Fock (RHF) energy gradient technique with the relativistic effective core potential (ECP) approximation[14a] and the GAUSSIAN80 program implemented with L. R. Kahn's ECP integral code.[14b] We adopted for the Pd atom, Hay and Wadt's relativistic ECP with valence double-ζ basis functions and for the Pt atom, Noell and Hay's relativistic ECP with valence double-ζ basis functions.[15] For CH_3 and CO the split-valence 3-21G basis was used.[16a] The 21G basis set was also adopted for hydride H, although a hydride bonded directly to a metal often required more flexible basis functions. In our previous studies of oxidative addition–reductive elimination and β-elimination, however, the same basis set has given good results.[12a,b] For PH_3 which is a "spectator" ligand not involved directly in the reaction, a smaller STO-2G basis set was used.[16b] During the geometry optimization, the structure of the complexes was assumed to maintain the C_s symmetry. This is reasonable as we are dealing with the group 10 d^8 complexes which should be square planar. We did not try to find tetrahedral structures. However, actual calculations with a small symmetry-breaking deformation from the C_s-optimized structures have created a force which retains the C_s symmetry.

To obtain better energetics, we also carried out the second-order Møller–Plesset perturbation (MP2) calculations at the RHF optimized geometries with a larger basis set, where Huzinaga–Dunning double-ζ

(7) (a) Attig, T. G.; Wojcicki, A. *J. Organomet. Chem.* **1974**, *82*, 397. (b) Reich-Rohrwig, P.; Wojcicki, A. *Inorg. Chem.* **1974**, *13*, 2457. (c) Davison, A.; Martinez, N. *J. Organomet. Chem.* **1974**, *74*, C17. (d) Flood, T. C.; Campbell, K. D. *J. Am. Chem. Soc.* **1984**, *106*, 2853. (e) Flood, T. C.; Campbell, K. D.; Downs, H. H.; Nakanishi, S. *Organometallics* **1983**, *2*, 1590. (f) Brunner, H.; Hammer, B.; Bernal, I.; Draux, M. *Organometallics* **1983**, *2*, 1595. (g) Wright, S. C.; Baird, M. C. *J. Am. Chem. Soc.* **1985**, *107*, 6899.

(8) Anderson, G. K.; Cross, R. J. *J. Chem. Soc., Dalton Trans.* **1979**, 1246.

(9) Ozawa, F.; Yamamoto, A. *Chem. Lett.* **1981**, 289.

(10) Garrou, P. E.; Heck, R. F. *J. Am. Chem. Soc.* **1976**, *98*, 4115.

(11) (a) Sakaki, S.; Kitaura, K.; Morokuma, K.; Ohkubo, K. *J. Am. Chem. Soc.* **1983**, *105*, 2280. (b) Berke, H.; Hoffmann, R. *J. Am. Chem. Soc.* **1978**, *100*, 7224.

(12) (a) Obara, S.; Kitaura, K.; Morokuma, K. *J. Am. Chem. Soc.* **1984**, *106*, 7482. (b) Koga, N.; Obara, S.; Kitaura, K.; Morokuma, K. *J. Am. Chem. Soc.* **1985**, *107*, 7109. (c) Han, J.; Fu, X. Y.; Liu, R. Z.; Koga, N.; Morokuma, K., to be published. (d) Nakamura, S.; Morokuma, K., to be published. (e) Upton, T. H.; Rappe, A. K. *J. Am. Chem. Soc.* **1985**, *107*, 1206. (f) Low, J. J.; Goddard, W. A., III. *J. Am. Chem. Soc.* **1984**, *106*, 6928. (g) Low, J. J.; Goddard, W. A., III. *J. Am. Chem. Soc.* **1984**, *106*, 8321. (h) Blomberg, M. R. A.; Brandemark, U.; Siegbahn, P. E. M. *J. Am. Chem. Soc.* **1983**, *105*, 5557.

(13) Koga, N.; Morokuma, K. *J. Am. Chem. Soc.* **1985**, *107*, 7230.

(14) (a) The RHF wave function can describe the electronic structure of the Pd(II) and Pt(II) complexes studied here, since they are formally in a low-spin d^8 electron configuration. The participation of a triplet state in the Pt reaction due to the strong spin-orbit coupling may have to be considered. However, a triplet unrestricted Hartree–Fock calculation at the RHF optimized transition state indicates that the triplet state is too high in energy to participate significantly. (b) Binkley, J. S.; Whiteside, R. A.; Krishnan, R.; Seeger, R.; DeFrees, D. J.; Schlegel, H. B.; Topiol, S.; Kahn, L. R.; Pople, J. A. *QCPE* **1981**, No. 406.

(15) (a) Hay, P. J.; Wadt, W. R. *J. Chem. Phys.* **1985**, *82*, 270. (b) Noell, J. O.; Hay, P. J. *Inorg. Chem.* **1982**, *21*, 14.

(16) (a) Binkley, J. S.; Pople, J. A.; Hehre, W. J. *J. Am. Chem. Soc.* **1980**, *102*, 939. (b) Hehre, W. J.; Stewart, R. F.; Pople, J. A. *J. Chem. Phys.* **1969**, *51*, 2657.

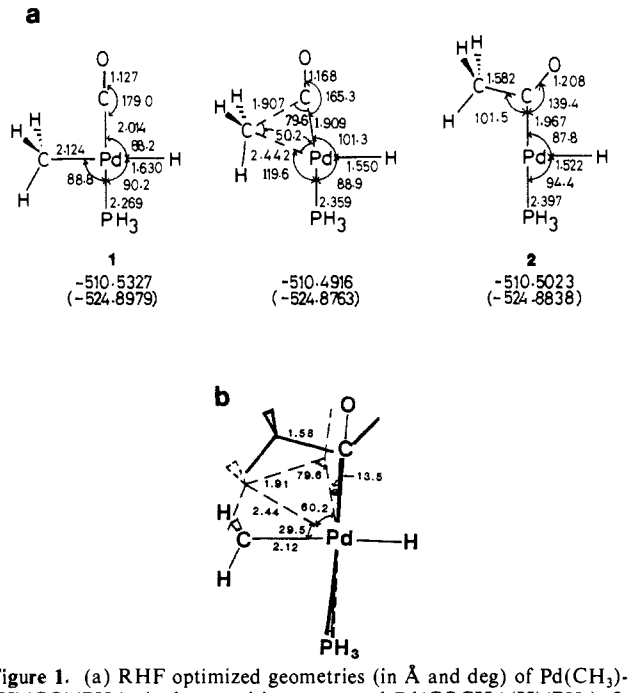

Figure 1. (a) RHF optimized geometries (in Å and deg) of $Pd(CH_3)(H)(CO)(PH_3)$, **1**, the transition state, and $Pd(COCH_3)(H)(PH_3)$, **2**. Total energies at the RHF and the MP2 (in parentheses) level are shown in hartree. (b) Optimized geometries superposed. The position of the Pd atom and the direction of the PdH bond are fixed. The illustrated positions of atoms are those in $Pd(CH_3)(H)(CO)(PH_3)$. The positions shown by the broken lines and the thick solid lines are those at the transition state and in $Pd(COCH_3)(H)(PH_3)$, respectively. For clarity, only essential geometrical parameters are shown.

basis functions were employed for all the ligands.[17]

For comparison, we have done similar calculations by using Hay and Wadt's ECP for the Pt atom.[15a] The energy profile obtained was similar to that reported here. The Pt ligand bond lengths except for Pt–CO were longer by about 0.1 Å. The Pt–CO bond was longer by about 0.2 Å. In the rest of the present paper we use only the Noell–Hay ECP for Pt.

Reaction of Pd Complex

In Figure 1, the optimized geometries of the reactant $Pd(CH_3)(H)(CO)(PH_3)$, **1**, the product $Pd(COCH_3)(H)(PH_3)$, **2**, and the transition state between them are shown.

Structures of $Pd(CH_3)(H)(CO)(PH_3)$ and $Pd(COCH_3)(H)(PH_3)_3$. The optimized structure of **1** is essentially square planar, as expected for a group 10 d^8 complex, all the ligand-Pd-ligand angles being about 90°. The bond distance of 2.124 Å between the methyl carbon atom and the Pd atom is close to Pd–C(sp^3) bond distances observed experimentally in divalent Pd complexes: 1.99 Å in $Pd\{CH_2C(=NN(CH_3)_2)C(CH_3)_3\}(acac)$,[18a] 2.14 Å in $Pd(CH_2COOCOCH_2)(PPh_3)_2$,[19a] and 2.09 Å in $Pd(CH_3)_2(PCH_3Ph_2)_2$,[18b] with a typical range thought to be 2.00–2.05 Å.[18c] The Pd–PH_3 bond distance of 2.269 Å is also in good agreement with the experimental Pd–P values: 2.33 Å in $Pd(CH_2COOCOCH_2)(PPh_3)_2$,[19a] 2.23 Å in $Pd(CH_2COO)(PPh_3)(Py)$,[19b] and 2.323 Å in $Pd(CH_3)_2(PCH_3Ph_2)_2$[18b] with a typical range thought to be 2.3–2.35 Å,[18c] though this agreement should not be taken too seriously as we have used a small basis set for PH_3. No experimental Pd–CO bond distance to be compared has been known, as the carbonyl–palladium complexes are too unstable for crystal structure determination.[18c]

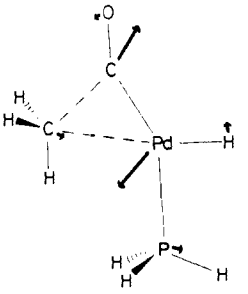

Figure 2. Forces acting on the atoms at the assumed transition state for carbonyl migration.

Though no three-coordinate acetyl–palladium complex, an unsaturated complex, has been isolated, the optimized geometry of **2** may be compared with known four-coordinate acyl–Pd(II) complexes, as **2** has the structure which can be considered to be derived from a four-coordinate planar complex by abstraction of a ligand. The structures of some aminoacyl complexes have been reported, in which the Pd–acyl carbon bond distance ranges from 1.94–2.00 Å,[20] in good agreement with the calculated distance. The location of the hydride, impossible to determine by the X-ray analysis, is not known, and thus the calculated Pd–H bond distances in **1** and **2** remain to be a prediction.

Transition State for Carbonyl Insertion Reaction. There are two or maybe three possible transition states, one for the CH_3 migration, one for the CO migration, and the other for concerted migration of both CO and CH_3. After extensive search starting from various initial guess geometries, we could obtain only one transition state shown in Figure 1. This is clearly the transition state for methyl migration. As seen in Figure 1, during the reaction the nonreacting PH_3–Pd–H portion of the complex changes the geometry only very slightly. At the transition state, the methyl group, with its pseudo C_3 axis kept nearly horizontal, has moved up half way toward the carbonyl group, the CH_3–Pd–PH_3 angle becoming larger by about 30° than in the reactant. The carbonyl group moves toward the methyl group slightly, the H–Pd–CO angle increasing by about 14°; it seems as if the carbonyl group is stretching an arm to accept the incoming methyl group. After the transition state, the methyl group proceeds further to the final position, while the carbonyl carbon snaps back toward the original position with the H–Pd–CO angle of about 90°.

When a chemical reaction is treated theoretically, it is convenient to calculate the reaction coordinate at the transition state. In this paper we have calculated an approximate reaction coordinate, which is the normal coordinate having the only imaginary normal frequency, obtained from the approximate second derivative matrix updated during the optimization steps. The main component of the approximate reaction coordinate, shown below, **5**, is the translation of the methyl group, confirming that this

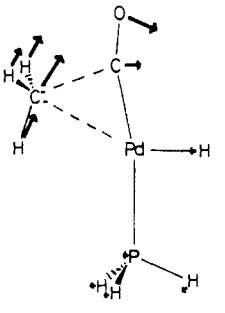

5

(17) Dunning, T. H.; Hay, P. J. In *Methods of Electronic Structure Theory*; Schaefer, H., Ed.; Plenum: New York, 1977; p 1.

(18) (a) Constable, A. G.; McDonald, W. S.; Sawkins, L. C.; Shaw, B. L. *J. Chem. Soc., Dalton Trans.* **1980**, *108*, 3487. (b) Wisner, J. M.; Bartczak, T. J.; Ibers, J. A.; Low, J. J.; Goddard, W. A., III. *J. Am. Chem. Soc.* **1986**, *108*, 347. (c) Maitlis, P. M.; Espinet, P.; Russell, M. J. H. In *Comprehensive Organometallic Chemistry*; Wilkinson, G., Stone, F. G. A., Abel, E. W., Eds.; Pergamon Press: Oxford, 1982; p 233.

(19) (a) Zenitani, Y.; Tokunan, H.; Kai, Y.; Yasuoka, N.; Kasai, N. *Bull. Chem. Soc. Jpn.* **1978**, *51*, 1730. (b) Kai, Y.; Yasuoka, N.; Kasai, N. *Bull. Chem. Soc. Jpn.* **1979**, *52*, 737.

(20) (a) Hegedus, L. S.; Anderson, O. P.; Zetterberg, K.; Allen, G.; Sirala-Hansen, K.; Olsen, D. J.; Packard, A. B. *Inorg. Chem.* **1977**, *16*, 1887. (b) Anderson, O. P.; Packard, A. B. *Inorg. Chem.* **1978**, *17*, 1333. (c) Anderson, O. P.; Packard, A. B. *Inorg. Chem.* **1979**, *18*, 1129.

structure is indeed the transition state connecting the reactant **1** and the product **2**. Both the transition-state structure and the direction of reaction coordinate unequivocally show that the reaction takes place through the methyl group migration.

In order to make certain that the carbonyl group does not migrate, we assume a transition state for carbonyl migration in which the angles CO–Pd–H and CH_3–Pd–PH_3 of the true transition state are exchanged, as shown in **6**. The forces acting on

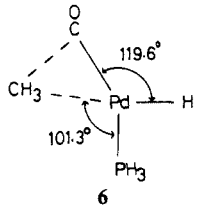

6

the atoms at the assumed transition state are shown in Figure 2. When geometry optimization is started at this point,[21] these forces immediately pushed the structure back to the true transition state. This test calculation and a failed extensive search strongly suggest that no transition states exist for the carbonyl migration nor for the concerted methyl and carbonyl migration. The assumed transition state **6** is less stable by about 7 kcal/mol than the true transition state. This instability is ascribed to the repulsion between carbonyl lone pair electrons and Pd d_{xy} electrons, as shown in **7**. The repulsion in the true transition state, as shown in **8**,

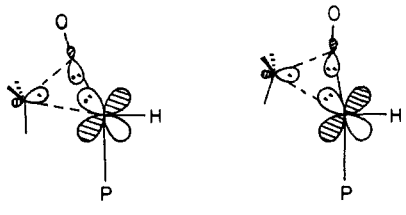

7 **8**

is weaker, because the carbonyl lone pair is no longer directed toward the Pd d_{xy} orbital and because the long distance and the small electron density (~1) keep an increase of the methyl sp^3 Pd d_{xy} repulsion to a minimum. The true transition state is also favorable because the Pd vacant $d_{x^2-y^2}$ orbital can overlap and mix nicely with the carbonyl lone pair orbitals. For this reason the alkyl group migration, not the carbonyl group migration, takes place. The alkyl group migration is expected to occur commonly in late transition-metal complexes.

Sakaki et al.[11a] have found the same conclusion as we obtained, the methyl migration being the easiest, and justified it as follows. They assumed a "transition state" which is located at the midpoint between the (unoptimized) transition state for methyl migration and that for CO migration, used the orbital mixing concept to look for the favorable direction of F and PH_3 motion, and found that F and PH_3 should move toward the direction where the Pt vacant d orbital directs toward the CO lone pair, which led to methyl migration. As discussed above, if one applies the orbital mixing concept directly to the motion of CH_3 and CO, one obtains the same conclusion, because, when one occupied d orbital is kept away from the CO lone pair to minimize the exchange repulsion, the vacant d orbital is directed to it to maximize orbital mixing.

During the course of the reaction, the Pd–PH_3 bond becomes longer, and the Pd–H bond becomes shorter. When the carbonyl group changes to an acyl group, its trans influence increases and lengthens the Pt–PH_3 bond from 2.269 to 2.397 Å. On the other hand, when the trans position of the hydride changes from CH_3 to a vacant site, the Pd–H bond becomes shorter by 0.11 Å. The trans influence/effect will be discussed in detail in a later section.

Recently, it has been proposed that the agostic interaction could assist the alkyl group migration.[22] The methyl in-plane CH bond

(21) The geometry optimization needs a starting geometry as an initial guess. Different starting geometries may lead to different transition states. As to the method of the geometry optimization see, also: Schlegel, H. B. *J. Comput. Chem.* **1982**, *3*, 214 and references cited therein.

Table I. Relative Energies (in kcal/mol) for the Process $M(CH_3)(H)(CO)(PH_3) \rightarrow M(COCH_3)(H)(PH_3)$

M	method	reactant	transtn state	product
Pd	RHF	0.0	25.8	19.1
	MP2[a]	0.0	13.5	8.8
Pt	RHF	0.0	31.3	23.0
	MP2[a]	0.0	21.8	17.6

[a] The geometries optimized with RHF are used.

Table II. Mulliken Population Analysis of $Pd(CH_3)(H)(CO)(PH_3)$, $Pd(COCH_3)(H)(PH_3)$, and the Transition State between Them

	reactant	transtn state	product
	Net Charge		
CH_3	−0.5704	−0.2673	−0.0923
CO	−0.1152	−0.3022	−0.4074
Pd	0.2017	0.0922	−0.0025
	Overlap Population[a]		
C1–C2	0.0491	0.2541	0.2261
Pd–C2	0.1436	−0.0705	−0.1691
Pd–C1	−0.3317	−0.1913	−0.0476

[a] C1 is the carbonyl carbon atom and C2 is the methyl carbon.

lengths of the product and the transition state are normal, i.e., 1.089 and 1.090 Å, respectively, and thus the agostic interaction[23] which would make the CH bond longer is absent. The electron-withdrawing CO group makes the electron-donating ability of the CH bond weaker, eliminating the CH → M donative agostic interaction.[23]

The activation barrier height calculated at the more reliable MP2 level (Table I) is 13.5 kcal/mol. Experimental activation enthalpy values for PtXR(CO)L and $Ir(Cl)_2(CF_3)(CO)(PPh_3)$ are 18.3–21.4[24,25] and 42.5 kcal/mol,[26] respectively. Considering the fact that carbonyl insertion takes place more easily for a Pd complex than for a Pt complex,[10] the calculated barrier height is quite reasonable.

Now we will discuss the change of electronic structure during the carbonyl insertion reaction. The results of Mulliken population analysis are shown in Table II. Although this analysis is not always reliable, it can provide a qualitative guide as to the change of electronic distribution during the reaction. In the course of reaction, the overlap population decreases between the Pd atom and the methyl group and increases between the methyl group and the carbonyl group, indicating that bond exchange is occurring smoothly. The overlap population between the Pd atom and the carbonyl carbon atom also increases, the Pd–CO bond becoming more covalent. As the reaction proceeds, the negatively charged methyl group in the reactant loses electrons to the carbonyl group, keeping the sum of CH_3 and CO electron population almost unchanged in the reactant and the product.

These circumstances become clearer with the analysis of the paired interactive hybrid molecular orbitals (IHMOs).[27] One can obtain pairs of fragment orbitals by diagonalizing $\mathbf{P}^+\mathbf{P}$, where **P** is the rectangular overlap population matrix between atomic orbitals of CH_3 and those of $Pd(H)(CO)(PH_3)$. After diagonalization, the overlap population matrix element is nonzero only within the pair and zero between orbitals in different pairs. Of these pairs, only a few with the largest eigenvalues, i.e., the largest overlap populations, play a dominant role in the interaction and thus are called IHMOs. In Figure 3, we show only the most

(22) Carmona, E.; Sanchez, L.; Marin, J. M.; Poveda, M. L.; Atwood, J. L.; Priester, R. D.; Rogers, R. D. *J. Am. Chem. Soc.* **1984**, *106*, 3214.
(23) (a) Brookhart, M.; Green, M. L. H. *J. Organomet. Chem.* **1983**, *250*, 395. (b) Koga, N.; Obara, S.; Morokuma, K. *J. Am. Chem. Soc.* **1984**, *106*, 4625. (c) Obara, S.; Koga, N.; Morokuma, K. *J. Organomet. Chem.* **1984**, *270*, C33.
(24) Glyde, R. W.; Mawby, R. J. *Inorg. Chem.* **1971**, *10*, 854.
(25) Wilson, C. J.; Green, M.; Mawby, R. J. *J. Chem. Soc., Dalton Trans.* **1974**, 421.
(26) Blake, D. M.; Winkelman, A.; Chung, Y. L. *Inorg. Chem.* **1975**, *14*, 1326.
(27) (a) Fujimoto, H.; Koga, N.; Fukui, K. *J. Am. Chem. Soc.* **1981**, *103*, 7452. (b) Fujimoto, H.; Yamasaki, T.; Mizutani, H.; Koga, N. *J. Am. Chem. Soc.* **1985**, *107*, 6157.

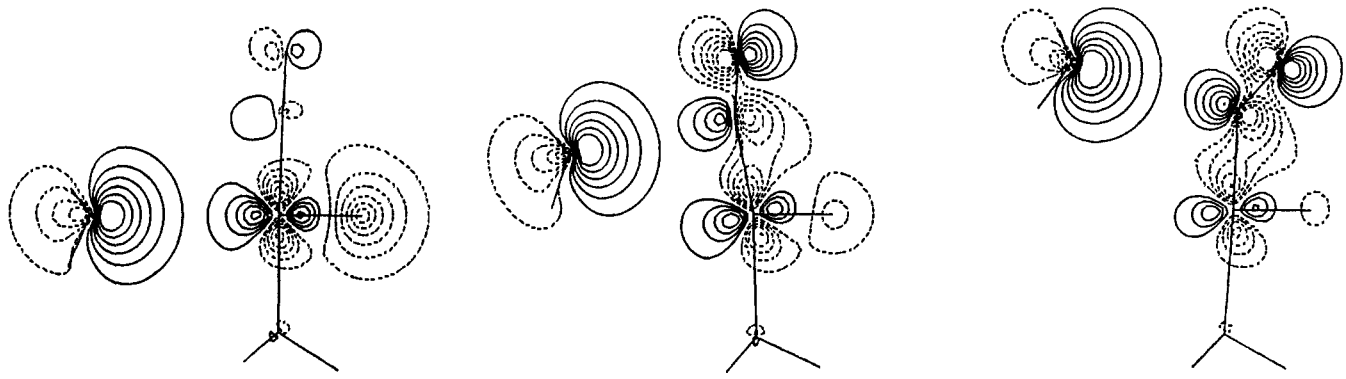

Figure 3. Interactive hybrid molecular orbitals of CH_3 and $Pd(H)(CO)(PH_3)$ for (left) the reactant, (middle) the transition state, and (right) the product. To avoid overcrowding of contours, the horizontal separation between the two fragments in the figure is taken to be larger than the real interfragment distance.

important pair of IHMOs for each geometry. That is to say, the dominant orbital interaction between the methyl group and the remaining part of the complex is condensed in this pair. Although the shape of the IHMO of the methyl group remains almost unchanged during the course of reaction, that of the $Pd(H)(CO)(PH_3)$ fragment changes smoothly. While the pair of the IHMOs for the reactant describes the CH_3–Pd bond and that for the product describes the CH_3–CO bond, the IHMO pair for the transition state has a character between the two and shows that the three-center transition state is stabilized by the bridging interaction of the methyl sp^3-like orbital between a Pd d orbital and the CO π^* orbital, leading to a low activation energy. This interaction should release the anionic character of the methyl group at the transition state.

The occupation number of each IHMO also demonstrates the change of the electronic structure. In general, when a covalent bond is formed, the occupation number of each orbital in the bond-forming pair is close to 1 with the sum for the pair close to 2. When the sum is over 2, the exchange repulsion is taking place between the orbitals in the pair; for a pure lone pair–lone pair exchange repulsion, the sum should be 4. A difference in occupancy in the pair, such as 1.5 on one orbital and 0.5 on the other, reflects an ionic character of the bond. The methyl IHMO decreases its occupation number from 1.5498 to 1.1028 upon going from the reactant to the transition state, indicating a decrease of anion character of the CH_3–Pd bond.

Reaction of Pt Complex

Structures of $Pt(CH_3)(H)(CO)(PH_3)$ and $Pt(COCH_3)(H)(PH_3)$. The optimized structures of the stationary points of the reaction 3 are shown in Figure 4. The Pt–CH_3 and Pt–PH_3 bond distances of **3** are in good agreement with those observed experimentally: for the Pt–CH_3 bond 2.12 Å in $Pt(CH_3)(ISO_2)(PPh_3)_2$,[28a] 2.08 Å in $Pt(CH_3)(Cl)(PCH_3Ph_2)$,[28b] 2.07 Å in $Pt(CH_3)(\eta\text{-}1\text{-}C_5H_5)(cod)$,[28c] 2.05 Å in $Pt(CH_3)(\eta\text{-}7\text{-}C_9F_6H_5)(cod)$,[28d] and 2.12 Å in $Pt(CH_3)_2(PCH_3Ph_2)_2$[18b] and for the Pt–P bond 2.284 Å in $Pt(CH_3)_2(PCH_3Ph_2)_2$.[18b] The Pt–CO bond length of 1.916 Å is within the range experimentally reported, 1.78–1.97 Å.[29] There is no experimental data of the Pt–H bond distance to be compared with.

As to the Pt–$COCH_3$ bond length of the product, the calculated result agrees well with that reported for a dinuclear complex, 1.972 Å in $Pt_2(\mu\text{-}Cl)_2(COC_2H_5)_2(P(CH_3)_2Ph)_2$.[30]

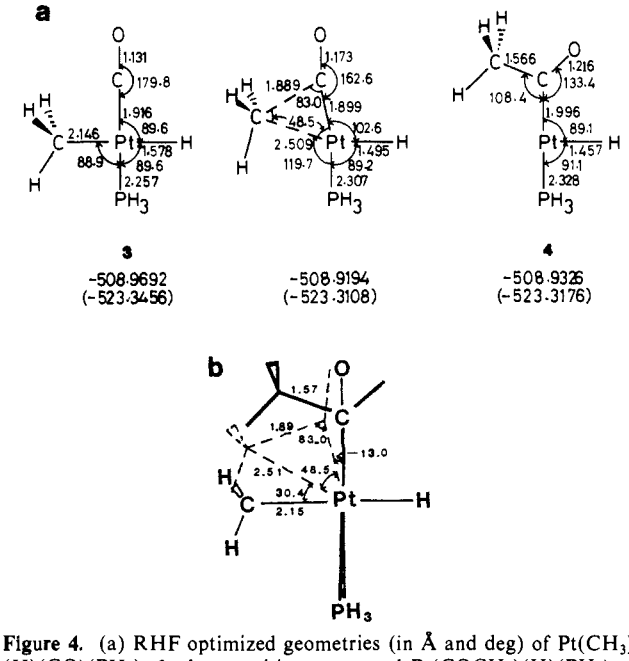

Figure 4. (a) RHF optimized geometries (in Å and deg) of $Pt(CH_3)(H)(CO)(PH_3)$, **3**, the transition state, and $Pt(COCH_3)(H)(PH_3)$, **4**. Total energies at the RHF and the MP2 (in parentheses) level are shown in hartree. (b) Optimized geometries superposed. See Figure 1 for convention.

Transition State for Carbonyl Insertion Reaction. The optimized transition-state structure (Figure 4) is very similar to that of the Pd complex (Figure 1), and the reaction mechanism is definitely the methyl group migration as in the case of the Pd complex. The change of the electronic structure throughout the reaction is also similar to the Pd case. At the transition state, the bridging interaction of the methyl sp^3-like orbital with the CO π^* and a Pt d orbital takes place.

The activation barrier calculated at the MP2 level is 21.8 kcal/mol (Table I), in good agreement with the experiment 4[25] where the rate-determining step is the first carbonyl "insertion" step, and the activation enthalpies are 19.4 and 21.4 kcal/mol in chlorobenzene and tetrahydrofuran, respectively.

$$Pt(C_2H_5)(Cl)(CO)(AsPh_3) \rightarrow Pt(COC_2H_5)(Cl)(AsPh_3) \xrightarrow{AsPh_3} Pt(COC_2H_5)(Cl)(AsPh_3)_2 \quad (4)$$

Comparison between the Reactions of the Pd and the Pt Complex

As summarized in Table I, the calculated activation barrier for carbonyl insertion of the Pd complex is lower by several

(28) (a) Snow, M. R.; Ibers, J. A. *Inorg. Chem.* **1973**, *12*, 224. (b) Bennett, M. A.; Chee, H.-K.; Robertson, G. B. *Inorg. Chem.* **1979**, *18*, 1061. (c) Day, C. S.; Day, V. W.; Shaver, A.; Clark, H. C. *Inorg. Chem.* **1981**, *20*, 2188. (d) Ibbott, D. G.; Payne, N. C.; Shaver, A. *Inorg. Chem.* **1981**, *20*, 2193.

(29) (a) Clark, H. C.; Corfield, P. W. R.; Dixon, K. R.; Ibers, J. A. *J. Am. Chem. Soc.* **1967**, *89*, 3360. (b) Albano, V. G.; Basso Ricci, G. M.; Bellon, P. L. *Inorg. Chem.* **1969**, *10*, 2109. (c) Field, J. S.; Wheatly, P. J. *J. Chem. Soc., Dalton Trans.* **1974**, 702. (d) Manojlovic-Muir, L.; Muir, K. W.; Walker, R. *J. Chem. Soc., Dalton Trans.* **1976**, 1279.

(30) Anderson, G. K.; Cross, R. J.; Manojlovic-Muir, L.; Muir, K. W.; Solomon, T. *J. Organomet. Chem.* **1979**, *170*, 385.

kcal/mol than that of the Pt complex. Garrou and Heck have found experimentally that the carbonyl insertion reaction of the Pd complex is about 180 times faster than that of the Pt complex.[10] Our present result agrees with this trend. Calderazzo proposed that this trend is due to a stronger metal–alkyl bond in the third-row transition-metal complex than in the second-row transition-metal complex.[3a] In fact, the endothermicity of the reaction of the Pt complex is calculated to be 18 kcal/mol at MP2, more endothermic than that of the Pd complex by 9 kcal/mol. The more endothermic the reaction is the higher the activation barrier would be. There are other experimental and theoretical evidences supporting the stronger Pt–C bond. Although no structure of a palladium–carbonyl complex has been determined experimentally, structures of several platinum–carbonyl complexes have been reported,[28] suggesting that the Pt–CO bond is stronger than the Pd–CO bond. An IR study has shown that the CO stretching frequency in the Pt complex is smaller than in the Pd complex,[31] suggesting that a strong π back donative interaction from metal to CO in the Pt complex leads to a weaker C–O bond and a stronger M–C bond. The calculated Pd–CO bond length of 2.014 Å is longer than the Pt–CO bond length of 1.916 Å (see Figures 1 and 4), maybe reflecting the bond energy difference, although the inclusion of the electron correlation may be necessary in order to obtain more accurate metal–carbonyl bond lengths.[32]

In order to assess the factors which cause a difference in the reactivity and the endothermicity between the Pd and the Pt complex, we estimated the difference in the bond strengths in the products and the reactants of both complexes. The bonds which are created or broken during the reaction are M–CH_3, M–CO, and M–$COCH_3$ bonds as well as a CO triple bond and a CH_3–CO bond. Since the difference in the behavior between the Pd and the Pt complex would be caused by the difference in the metal–ligand bonds, we pay direct attention to the M–CH_3, M–CO, and M–$COCH_3$ bonds, while the effects of CH_3–CO and CO bond strengths are implicitly considered. As the calculation at the present level cannot give quantitative bond energies, we evaluate only the differences between the Pd and the Pt complexes.[33]

At first we show the way in which the binding energy differences between the Pd and the Pt complex were calculated. There are two theoretical ways, A and B, through which $M(CH_3)(H)(CO)(PH_3)$ is formally constructed from $M(PH_3)$, CO, and CH_4 fragments.

A:

$$M(PH_3) + CO \rightarrow M(CO)(PH_3) + \Delta E(M, A\text{-}1)$$

$$M(CO)(PH_3) + CH_4 \rightarrow M(CH_3)(H)(CO)(PH_3) + \Delta E(M, A\text{-}2)$$

B:

$$M(PH_3) + CH_4 \rightarrow M(CH_3)(H)(PH_3) + \Delta E(M, B\text{-}1)$$

$$M(CH_3)(H)(PH_3) + CO \rightarrow M(CH_3)(H)(CO)(PH_3) + \Delta E(M, B\text{-}2)$$

By using the energy changes calculated above, one can calculate the binding energy differences as follows

$$D_e(Pt\text{–}CO) - D_e(Pd\text{–}CO) = \Delta E(Pt, A\text{-}1) - \Delta E(Pd, A\text{-}1) \text{ or } \Delta E(Pt, B\text{-}2) - \Delta E(Pd, B\text{-}2)$$

Though this energy difference is designated as the difference in the M–CO bond energy, it includes implicitly a negative of the difference in the CO bond energy in the complex as well. Similarly,

$$D_e(Pt\text{–}CH_3) - D_e(Pd\text{–}CH_3) = \Delta E(Pt, A\text{-}2) - \Delta E(Pd, A\text{-}2) - (D_e(Pt\text{–}H) - D_e(Pd\text{–}H)) \text{ or } \Delta E(Pt, B\text{-}1) - \Delta E(Pd, B\text{-}1) - (D_e(Pt\text{–}H) - D_e(Pd\text{–}H))$$

The binding energy difference of the metal hydride bond was calculated as follows

$$D_e(Pt\text{–}H) - D_e(Pd\text{–}H) = (\Delta E(Pt, C) - \Delta E(Pd, C))/2 \text{ or } (\Delta E(Pt, D) - \Delta E(Pd, D))/2$$

where ΔE(M, C) and ΔE(M, D) (M = Pt and Pd) are the energy changes of the following reactions.

C:

$$M(CO)(PH_3) + H_2 \rightarrow M(H)_2(CO)(PH_3) + \Delta E(M, C)$$

D:

$$M(PH_3) + H_2 \rightarrow M(H)_2(PH_3) + \Delta E(M, D)$$

Similarly, we calculated the M–$COCH_3$ bond energy difference between the Pd and the Pt complex. Consider the following chemical process

E:

$$M(PH_3) + CH_3CHO \rightarrow M(COCH_3)(H)(PH_3) + \Delta E(M, E)$$

Thus

$$D_e(Pt\text{–}COCH_3) - D_e(Pd\text{–}COCH_3) = \Delta E(Pt, E) - \Delta E(Pd, E) - (D_e(Pt\text{–}H) - D_e(Pd\text{–}H))$$

Here again the calculated Pt–$COCH_3$ energy difference contains

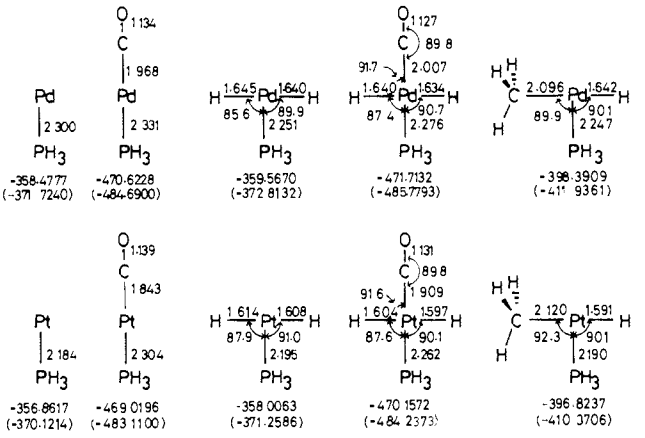

Figure 5. Optimized geometries (in Å and deg) of $M(PH_3)$, $M(CO)(PH_3)$, $M(H)_2(PH_3)$, $M(H)_2(CO)(PH_3)$, and $M(CH_3)(H)(PH_3)$ (M = Pd, Pt). Total energies at the RHF and the MP2 (in parentheses) level are shown in hartree.

Table III. Energy Changes, ΔE(M,n), of Chemical Processes Used for Calculation of Difference of Bond Strengths[a] (in kcal/mol)

	RHF		MP2	
n	M = Pd	M = Pt	M = Pd	M = Pt
A-1	32.5	40.5	49.0	63.0
A-2	−42.1	−17.1	−43.9	−26.4
B-1	−40.0	−9.3	−41.2	−18.0
B-2	30.4	32.7	46.3	54.5
C	−20.4	9.2	−27.7	−3.7
D	−21.1	13.6	−27.7	2.4
E	−19.3	9.8	1.1	23.9

[a] The energies of CO, CH_4, CH_3CHO, and H_2 at the RHF level are −112.0933, −39.9769, −152.0553, and −1.1230 hartree, respectively (Whiteside, R. A.; Frisch, M. J.; Binkley, J. S.; DeFrees, D. J.; Schlegel, H. B.; Raghavachari, K.; Pople, J. A. Carnegie-Mellon Quantum Chemistry Archiv, Carnegie-Mellon University, 1981). Those at the MP2 level are −112.8880, −40.2779, −153.1582, and −1.1334 hartree.

(31) Calderazzo, F.; Dell'Amico, D. B. *Inorg. Chem.* **1981**, *20*, 1310 and references cited therein.
(32) Hay, J. P.; Wadt, W. R. *J. Chem. Phys.* **1985**, *83*, 4641.
(33) In a free transition-metal atom, several electronic states lie energetically close to each other. In the case of a transition-metal complex with a single ligand, the character of a metal–ligand bond is sensitive to the energy level of atomic states, and thus a high quality computational method has to be used. On the other hand, when many ligands are complexed to a central metal, as in the present systems, the ligand field effect causes a large separation between the states. In such a case, it is expected that the basis set and the computational method used here give a correct description of the bonding character.[12]

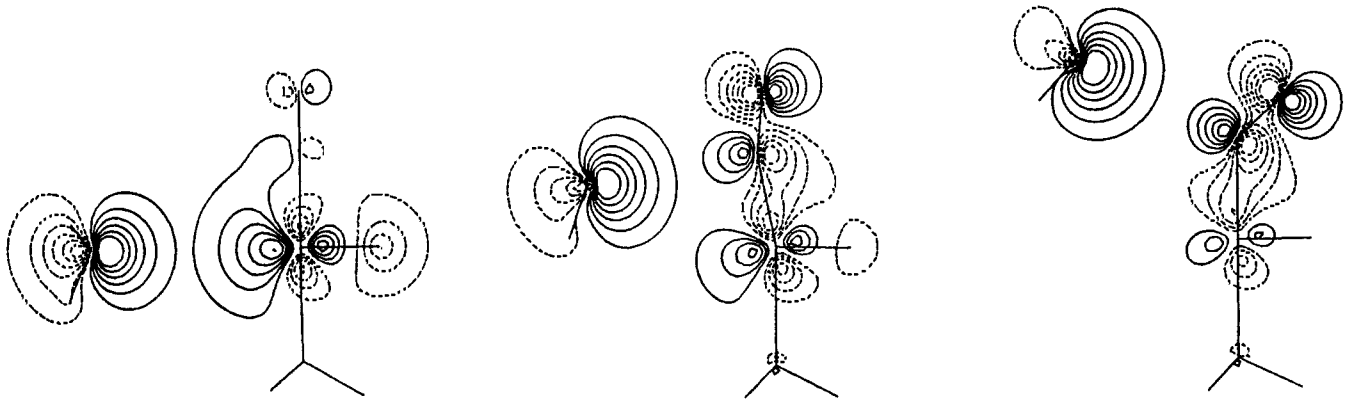

Figure 6. Interactive hybrid molecular orbitals of CH_3 and $Pt(H)(CO)(PH_3)$ for (left) the reactant, (middle) the transition state, and (right) the product. To avoid overcrowding of contours, the horizontal separation between the two fragments in the figure is taken to be larger than the real interfragment distance.

Table IV. Difference of Bond Strengths of M–L[a] between Pd and Pt Complexes (in kcal/mol)[b]

	RHF			MP2		
L	I	II	(I + II)/2	I	II	(I + II)/2
CH_3	10.2	13.3	11.7	5.5	8.1	6.8
CO	8.0	2.3	5.2	14.0	8.2	11.2
$COCH_3$	14.3	11.7	13.0	10.8	7.7	9.2

[a] D_e(Pt–L) − D_e(Pd–L). [b] Processes A and C are used for I and B and D for II. D_e(Pt–H) − D_e(Pd–H) = 14.8 and 17.4 kcal/mol for I and II, respectively, at the RHF level, and 12.0 and 15.1 kcal/mol at the MP2 level.

implicitly the difference in the CO and other bond energy within $COCH_3$. In calculating the energies of the complexes which appear in the above equations, all the geometries were optimized. The optimized geometries are shown in Figure 5 and the values of ΔE(M,n) in Table III.

The results, shown in Table IV, clarify the differences between the Pd and the Pt complex. All the metal–carbon bonds are stronger in the Pt complex than in the Pd complex. In the Pt complex there are two stronger bonds, Pt–CH_3 by 7 kcal/mol and Pt–CO by 11 kcal/mol, in the reactant and one stronger bond, Pt–$COCH_3$ by 9 kcal/mol, in the product. Therefore, the reaction of the Pt complex is more endothermic by 11 + 7 − 9 = 9 kcal/mol at the more reliable MP2 level and thus requires a larger activation energy.

Probably, this difference of the bond strengths can be ascribed to the relativistic effect which is larger in the Pt atom than that in the Pd atom. Two seemingly different explanations have been proposed for the relativistic effect on bonding. The first approach utilizes the fact that the relativistic effect makes an atomic s orbital more contracted and a d orbital more diffuse. Such changes of atomic orbitals result in a change in the bond length of the complex.[34a] In the second approach, the relativistic effect is due to the change of the potential energy curve caused by the relativistic change of the Hamiltonian and has nothing to do with orbital changes.[34b] Schwartz et al., however, have argued that two explanations are equivalent,[34c] but a recent paper favors the first approach.[34d]

In this section we used the first approach for the discussion. The relativistic effect makes the d atomic orbital higher in energy and more diffuse in space and the s atomic orbital lower in energy and more contracted in space.[34a] In a carbonyl complex, the back donation makes an important contribution to the metal–carbonyl bond. The expansion of d atomic orbitals in the Pt complex leads to a larger overlap between metal d orbitals and the carbonyl π^* orbital. Such a larger overlap could make the back donative interaction more favorable and thus the Pt–CO bond stronger. In the acetyl complex, of course, there is a back donative interaction from a metal d orbital to π^* of the acetyl group. In addition, the metal–acetyl σ orbital could be made stronger by the relativistic effect; the energy lowering of the s atomic orbital enhances its participation in the metal ligand bond, allowing an sd hybridized orbital formed and directed to the acetyl group. The same effect would make a Pt–CH_3 bond stronger.

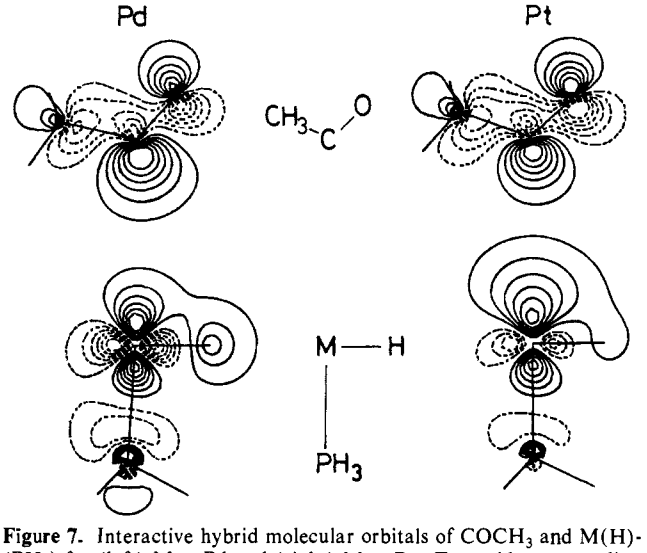

Figure 7. Interactive hybrid molecular orbitals of $COCH_3$ and $M(H)(PH_3)$ for (left) M = Pd and (right) M = Pt. To avoid overcrowding of contours, the vertical separation between the two fragments in the figure is taken to be larger than the real interfragment distance.

In Figure 6, we show the IHMOs for the reaction of the Pt complex. They are very similar to those of the Pd complex in Figure 3 except for the reactant IHMOs describing the Pt–CH_3 bond. In the Pt fragment, the s character of the IHMO is more pronounced than in the Pd fragment, consistent with the above discussion.[35]

The enhanced s character of Pt seems to affect the structure of the Pt–$COCH_3$ moiety; the M–C–C bond angle of the product acetyl complex is 102° for Pd and 108° for Pt. To clarify this difference, we have calculated in Figure 7 the IHMOs representing the orbital interaction between the CH_3CO fragment and the $M(H)(PH_3)$ fragment. A comparison shows that the Pd orbital for this bond is almost purely d in character, whereas the Pt orbital for the bond contains a small but significant s character, consistent again with the above discussion. Therefore, in the Pd–acetyl

(34) (a) Pyykkö, P.; Desclaux, J.-P. *Acc. Chem. Res.* **1979**, *12*, 276. (b) Ziegler, T.; Snijders, J. G.; Baerends, E. J. *J. Chem. Phys.* **1981**, *74*, 1271. (c) Schwarz, W. H. E.; Chu, S. Y.; Mark, F. *Mol. Phys.* **1983**, *50*, 603. (d) Christiansen, P. A.; Ermler, W. C. *Mol. Phys.* **1985**, *55*, 1109.

(35) An analysis of GVB wave functions has given a similar result.[18b]

Table V. Substituent Effect on Relative Energies (in kcal/mol) for the Process $Pd(R)(CO)(H)(PH_3) \rightarrow Pd(COR)(H)(PH_3)$[a]

R	Pd(R)(CO)-(H)(PH_3)	transtn state	Pd-(COR)-(H)(PH_3)
CH_3	0.0	25.8	19.1
CHF_2[b]	0.0	40.9	31.2
C_2H_5[b]	0.0	23.1	14.6

[a] Obtained with RHF. [b] The geometries optimized for R = CH_3 are used.

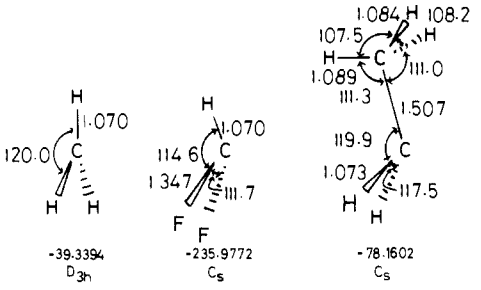

Figure 8. Optimized geometries of CH_3, CHF_2, and C_2H_5 (in Å and deg). Total energies at the RHF level are shown in hartree.

complex, a direct interaction, **9**, of a d orbital lobe with the σ orbital of the methyl group may take place.

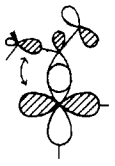

9

Substituent Effect

In order to investigate the effect of alkyl group substituent on the reaction, we use the difluoromethyl and ethyl group as migrating groups in the Pd complex.

$$Pd(R)(H)(CO)(PH_3) \rightarrow Pd(COR)(H)(PH_3) \quad (5, 6)$$

10: R = CHF_2 **11**: R = CHF_2
12: R = CH_2CH_3 **13**: R = CH_2CH_3

In the former the fluorine is an electron-withdrawing substituent, and in the latter the methyl substitution is an introduction of an electron-releasing substituent. In this section, calculations were carried out only with the RHF method so as to obtain qualitative results. The geometries of the stationary points are not optimized but were taken from those of **1** by simply replacing methyl hydrogen atom(s) by a methyl group or fluorides having a standard geometry.

The energy profiles obtained are shown in Table V. The fluoromethyl migration has a higher activation barrier by 15 kcal/mol and is more endothermic by 12 kcal/mol than the methyl migration, while the ethyl migration has a lower activation energy by 3 kcal/mol and is less endothermic by 4 kcal/mol. One finds a trend that the more electron-withdrawing the substituent on the migrating group is, the higher the activation barrier is, in agreement with the experimental findings. For instance, in the reaction of $Pd(Ph)(X)(PR_3)_2$ with CO, an electron-withdrawing substituent on the para position of phenyl decreases the reaction rate, and an electron-releasing substituent increases it.[10] In the carbonyl insertion reaction of $RMn(CO)_5$, the correlation between the reaction rate and the alkyl group has been investigated,[36] and it was found that the reaction rate decreases in the order of $C_2H_5 > CH_3 > CH_2F$, with which the trend found here agrees well. One also finds another trend in the calculated results that the more electron-withdrawing the alkyl group is, the more endothermic the reaction is. This has been found experimentally in the equilibrium of $Rh(Cl)_2(COR)(PPh_3)_2 \leftrightarrow Rh(Cl)_2(CO)(R)(PPh_3)$;[5] the equilibrium constant was 0.29 for R = CH_3, <0.02 for R = C_2H_5, and >40 for R = CH_2Cl.

(36) Calderazzo, F., Noack, K. *Coord. Chem. Rev.* **1966**, *1*, 118.

Table VI. Substituent Effect on the Difference of Bond Strengths in Pd Complexes (in kcal/mol)[a]

	R	
	CHF_2	C_2H_5
$D_e(Pd-CH_3) - D_e(Pd-R)$	−4.0	4.8
$D_e(CO-CH_3) - D_e(CO-R)$	8.1	0.3

[a] Calculated with RHF. $\Delta E(F) = -7.5$ kcal/mol, $\Delta E(G) = 2.5$ kcal/mol, $\Delta E(H) = 4.7$ kcal/mol, and $\Delta E(I) = -2.0$ kcal/mol. $D_e(CHF_2-H) - D_e(CH_3-H) = -3.5$ kcal/mol and $D_e(C_2H_5) - D_e(CH_3-H) = -2.3$ kcal/mol.

Table VII. Trans Effect Represented by Relative Energies (in kcal/mol) for the Process **14** → **15**[a] Compared with **1** → **2**[a]

	reactant	transtn state	product
1 → **2**	0.0	25.8	19.1
14 → **15**	0.0	27.3	19.3

[a] Calculated with RHF. Geometries are all optimized.

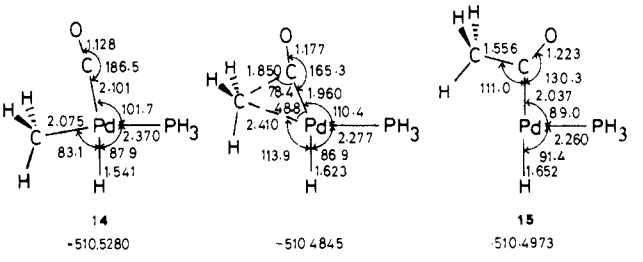

Figure 9. Optimized geometries (in Å and deg) of $Pd(CH_3)(H)(CO)(PH_3)$, **14**, the transition state, and $Pd(COCH_3)(H)(PH_3)$, **15**. Total energies at the RHF level are shown in hartree.

In order to analyze the effect of the substituent, we calculated the bond strength differences between Pd–R (R = CHF_2, C_2H_5) and Pd–CH_3 and between PdCO–R (R = CHF_2, C_2H_5) and PdCO–CH_3, adopting the following procedure.

$$Pd(CH_3)(CO)(PH_3) + R-H \rightarrow Pd(R)(CO)(PH_3) + CH_4 + \Delta E(m)$$

R = CHF_2 (m = F)
R = C_2H_5 (m = G)

$$Pd(COCH_3)(PH_3) + R-H \rightarrow Pd(COR)(PH_3) + CH_4 + \Delta E(n)$$

R = CHF_2 (n = H)
R = C_2H_5 (n = I)

Therefore

$$D_e(Pd-CH_3) - D_e(Pd-R) = \Delta E(m) - (D_e(R-H) - D_e(CH_3-H))$$

$$D_e(Pd-COCH_3) - D_e(Pd-R) = \Delta E(n) - (D_e(R-H) - D_e(CH_3-H))$$

where

$$D_e(R-H) - D_e(CH_3-H) = (E(R) - E(R-H)) - (E(CH_3) - E(CH_4))$$

The geometries of CH_3 and R are optimized with the open shell RHF method shown in Figure 8. The results of analysis are shown in Table VI. The Pd–CHF_2 bond is the strongest, and the Pd–C_2H_5 bond is the weakest among the three Pd–R bonds. This difference makes a contribution to the difference in endothermicity. In addition, the weakness of the CO–CHF_2 bond also contributes to the large endothermicity of the reaction 5, while the strength of CO–C_2H_5 bond is almost the same as CO–CH_3.

As shown in the preceding section, the methyl group in the reactant has a negative charge. Electron-withdrawing fluorines stabilize the negative alkyl group to make the Pd–R bond stronger.

Scheme II

$CH_3CO \overset{2.037}{—} Pd \overset{1.652}{—} H$	in	**15**
$CH_3 \overset{2.124}{—} Pd \overset{1.630}{—} H$		**1**
$OC \overset{2.101}{—} Pd \overset{1.541}{—} H$		**14**
$CH_3CO \overset{1.967}{—} Pd \overset{2.397}{—} PH_3$		**2**
$CH_3 \overset{2.075}{—} Pd \overset{2.370}{—} PH_3$		**14**
$OC \overset{2.014}{—} Pd \overset{2.269}{—} PH_3$		**1**

On the other hand, the electron-releasing methyl group produces a reverse effect.

Trans Effect

Often a matter of concern are effects of the trans ligand on the reaction rate and the structure of the complex, called the trans effect and the trans influence, respectively. In this section, for simplicity, we call them altogether the trans effect. In the present system, the ligands which affect the structure and the reaction are the hydride and PH_3. Thus, we studied the reaction of the Pd complex in which the position of H and PH_3 are switched from those of **1**. The RHF optimized structures of the reactant, the transition state, and the product are shown in Figure 9. The energy profile calculated at the RHF level is shown in Table VII and compared with that of **1**. As shown in Figures 1 and 9, the structures of **2** and **15** are square planar, three coordination sites

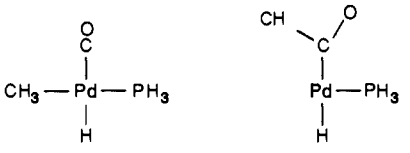

14

15

(7)

being occupied by ligands and the remaining one being empty. By taking an "empty" ligand into account, one can specify the trans position of each ligand and discuss the trans effect in three coordinate complexes.

First, we show in Scheme II (in unit of Å) a comparison of the optimized geometrical parameters between the reference, **1** and **2**, and the switched, **14** and **15**. Comparing PH_3 and hydride, the hydride makes the bond length between Pd and the trans ligand longer. For instance, the CH_3–Pd bond length trans to H in **1** is longer than that trans to PH_3 in **14** by 0.05 Å. The hydride has a stronger trans effect than PH_3. If one compares the trans effect of CH_3CO, CH_3, and CO on Pd–H and Pd–PH_3 bond lengths, one sees that the effect decreases in the order CH_3CO > CH_3 > CO. The trans effect can also be seen in the structure of the transition states in Figures 1 and 9. The Pd–CO bond length is longer and the Pd–CH_3 bond length is shorter in the transition state of **14** than in the transition state of **1**.

The activation barrier of the reaction of **14** is higher by 2.5 kcal/mol than that of the reaction of **1**. The strong trans effect of the hydride makes the Pd–CH_3 bond weaker, leading to a lower activation barrier. This trend is in agreement with Ozawa and Yamamoto's experiment that *cis*-$Pd(CH_3)_2(L)_2$ (L = PR_3) reacts more slowly with CO than *trans*-$Pd(CH_3)_2(L)_2$.[9] The endothermicity of the reaction, however, changes little by switching the hydride and PH_3. Apparently the trans effects on the M–CH_3 and the M–$COCH_3$ bond strengths cancel out with each other.

In **14**, the PH_3–Pd–CO bond angle is larger by 10° than the corresponding H–Pd–CO angle of **1**. Since the weak Pd–CO bond is further weakened due to the strong trans effect of hydride, the steric hindrance by PH_3 probably easily opens up the PH_3–Pd–CO angle. On the other hand, the strong Pd–$COCH_3$ bond maintains the PH_3–Pd–CO bond angle close to 90° in **15**.

The Pd–C–C angle of **15** is 111°, larger than that of **2** and close to that of **4**. The Pd–$COCH_3$ bond of **15** is mainly of d character. However, due to the strong trans effect of hydride, covalency of the Pd–$COCH_3$ bond becomes weaker. That is, the weight of d orbital in Pd–$COCH_3$ bonding is smaller as shown in **16**. Thus, the overlap between CH_3 and the Pd d orbital is smaller to lead to a weak CH_3–Pd interaction.

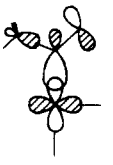

16

Conclusions

We studied the carbonyl insertion reaction of $Pd(CH_3)(H)(CO)(PH_3)$ and $Pt(CH_3)(H)(CO)(PH_3)$ by using an ab initio MO method with energy gradient. All the structures of the stationary points were optimized. The transition state structures obtained for both complexes indicate that the reaction path is the methyl group migration through a three-center transition state. Although the structures of Pd and Pt complexes are very similar to each other, the activation barrier is higher, and the reaction is more endothermic for the Pt complex than for the Pd complex. This has been ascribed to differences in metal–ligand bond strengths; all the platinum–carbon bonds (Pt–CH_3 and Pt–CO in the reactant and Pt–$COCH_3$ in the product) are stronger than the corresponding palladium–carbon bonds. Substitution on the migrating methyl group changes the reaction energy profile. Fluorine substitution makes the reaction unfavorable, strengthening the metal–alkyl bond. Methyl substitution produces a reverse effect. The trans effect on the metal–CH_3 bond makes it weaker to give a lower activation energy.

Acknowledgment. We are grateful to Prof. A. Yamamoto for stimulating discussions and encouragement and to Dr. S. Nakamura for valuable comments and discussions. The calculations were carried out at the IMS Computer Center.

Registry No. **1**, 99248-77-8; **2**, 99248-78-9; **3**, 99248-79-0; **4**, 103835-72-9; **10**, 103835-73-0; **12**, 103835-74-1; **14**, 103883-00-7; Pd(COCHF$_2$)(H)(PH_3), 103835-75-2; Pd($COCH_2CH_3$)(H)(PH_3), 103835-76-3.